similar to that of Cr(VI) under the same conditions of pH.

We are continuing to investigate the chemical, electrochemical, and analytical properties of these and related Cr(V) complexes.

Registry No. I^-, 84622-43-5; II^-, 89194-74-1; III^-, 108591-78-2; I^{2-}, 99495-02-0; II^{2-}, 89194-74-1; III^{2-}, 108591-79-3; II, 108591-80-6; acetic acid, 64-19-7.

Department of Inorganic Chemistry
The University of Sydney
Sydney, NSW 2006, Australia

James M. Eckert
Robert J. Judd
Peter A. Lay*

Received October 31, 1986

Iron-57 Hyperfine Splitting and Rhombic Field Orientation in Low-Spin Ferric Heme Complexes

Sir:

We wish to report the angular orientation of a rhombic crystal field that has been determined for the first time from frozen-solution EPR measurements on ^{57}Fe-substituted low-spin Fe(III) heme complexes, $Fe(TPP)(OMe)_2^-$ and Fe(TPP)(SEt)(MeOH), where TPP is the tetraphenylporphyrin dianion. The analysis of hyperfine (hf) splittings due to the ^{57}Fe nucleus ($I = {}^1/_2$) enables us also to determine the relative orientations of **g** and hf tensors and the sign of the **g** tensor determinant. The rhombic field orientation is closely related to the rotational orientation of axial ligand(s) and, as such, is important in a detailed understanding of structure–reactivity relationships in hemoproteins and their models. Special attention has been drawn to this subject in recent X-ray,[1,2] NMR,[3] EPR,[4] and MO calculation[2] studies.

The second-derivative curves of frozen-solution spectra observed for $^{57}Fe(TPP)(OMe)_2^-$ (**1**) and ^{57}Fe(TPP)(SEt)(MeOH) (**2**) are shown in Figures 1 and 2, respectively. The hf splitting value ($A_{(i)}$) in the g_i absorption peak was obtained by a computer simulation based on the line shape for the corresponding ^{56}Fe species, where g_i and i (=X, Y, Z) refer to the principal value and axis of **g** tensor, respectively. The observed values $A_{(i)}$ and $|g_i|$ are summarized in Table I. Remarkable differences in $A_{(X)}$ and $A_{(Y)}$ between **1** and **2** are noticed.

To interpret such observed differences, we have evaluated $A_{(i)}$ theoretically. We assume, in analogy with single-crystal results on low-spin hemoproteins[5] and model complexes,[6] that $|g_Z| > |g_Y| > |g_X|$ and that the Z axis lies along the heme normal. Further, the cubic field is assumed to be much stronger than the low-symmetry field. We then deal with the case in which the axes of the rhombic component field are rotated about the heme normal by an angle φ. It can be shown, according to Oosterhuis and Lang,[7] that the principal axes of **g** and hf tensors rotate about the heme normal by angles φ_g and φ_A, respectively, while the cubic axes (x, y, z) remain fixed to the heme coordinate system (Figure 3). With the lowest Kramers doublet for the $t_2^5\ ^2T_2$ state,[8] $\Psi^{\pm}$

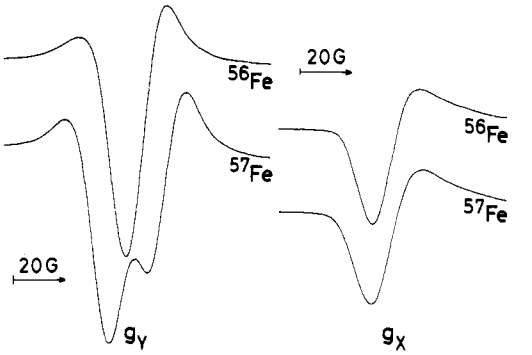

Figure 1. ^{57}Fe hf splittings observed for $Fe(TPP)(OMe)_2^-$ (**1**) in CH_2Cl_2–CD_3OD (1:1 v/v) at 20 K. The second-derivative curves of the g_X and g_Y absorption peaks are compared between the ^{57}Fe (95.15% enriched) and ^{56}Fe (in natural abundance) species. The scale is adjusted so that the two curves have the same height. The sample solution was prepared in situ by adding 50 equiv of CD_3ONa to 1.4 mM solution of ^{57}Fe- or ^{56}Fe(TPP)Cl in CH_2Cl_2–CD_3OD. The deuterium substitution resulted in a slight narrowing of the line width.

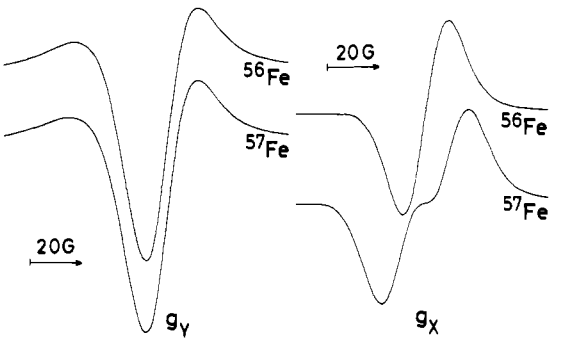

Figure 2. ^{57}Fe hf splittings observed for Fe(TPP)(SEt)(MeOH) (**2**) in CH_2Cl_2–MeOH (3:1 v/v) at 20 K. The second-derivative curves of the g_X and g_Y absorption peaks are compared between the ^{57}Fe (95.15% enriched) and ^{56}Fe (in natural abundance) species. The scale is adjusted so that the two curves have the same height. The sample solution was prepared in situ by adding 15 equiv of EtSH to 1.4 mM solution of ^{57}Fe- or ^{56}Fe(TPP)(OMe) in CH_2Cl_2–MeOH. **2** is formed according to Fe(TPP)(OMe) + EtSH → Fe(TPP)(SEt) + MeOH → **2**. The deuterium substitution was not undertaken.

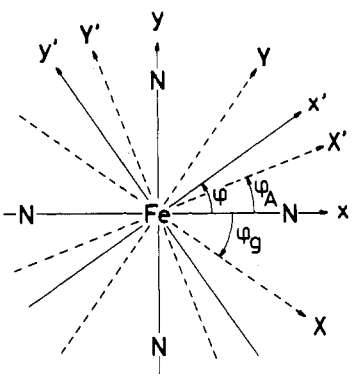

Figure 3. Angular orientation of the principal axes of the **g** tensor (X, Y, Z), hf tensor (X', Y', Z'), and low-symmetry field (x', y', z') with respect to the cubic field axes (x, y, z), which remain fixed to the heme coordinate system.

$= A(\cos\varphi|\pm{}^1/_2\xi\rangle - \sin\varphi|\pm{}^1/_2\eta\rangle) \pm iB(\sin\varphi|\pm{}^1/_2\xi\rangle + \cos\varphi|\pm{}^1/_2\eta\rangle) \pm C|\mp{}^1/_2\zeta\rangle$, we find that

$$\varphi_g = -\varphi \tag{1}$$

and

$$\tan 2\varphi_A = -(E - F)\tan 2\varphi/(E + F) \tag{2}$$

together with the expressions for g_i and $A_{(i)}$ given as

(1) Geiger, D. K.; Lee, Y. J.; Scheidt, W. R. *J. Am. Chem. Soc.* **1984**, *106*, 6339.
(2) Scheidt, W. R.; Chipman, D. M. *J. Am. Chem. Soc.* **1986**, *108*, 1163.
(3) Walker, F. A.; Buehler, J.; West, J. T.; Hinds, J. L. *J. Am. Chem. Soc.* **1983**, *105*, 6923.
(4) Walker, F. A.; Huynh, B. H.; Scheidt, W. R.; Osvath, S. R. *J. Am. Chem. Soc.* **1986**, *108*, 5288.
(5) Helcke, G. A.; Ingram, D. J. E.; Slade, E. F. *Proc. R. Soc. London, B* **1968**, *169*, 275. Hori, H. *Biochim. Biophys. Acta* **1971**, *251*, 227. Mailer, C.; Taylor, C. P. S. *Can. J. Biochem.* **1972**, *50*, 1048.
(6) Byrn, M. P.; Strouse, C. E. *J. Am. Chem. Soc.* **1981**, *103*, 2633. Byrn, M. P.; Katz, B. A.; Keder, N. L.; Levan, K. R.; Magurany, C. J.; Miller, K. M.; Pritt, J. W.; Strouse, C. E. *Ibid.* **1983**, *105*, 4916.
(7) Oosterhuis, W. T.; Lang, G. *Phys. Rev.* **1969**, *178*, 439.
(8) $|\pm{}^1/_2\gamma\rangle = |t_2^5\ ^2T_2 \pm {}^1/_2\gamma\rangle$ ($\gamma = \xi, \eta, \zeta$). Note that the transformation properties of γ are defined in the x, y, z coordinate system, while $\pm{}^1/_2$ refer to the spin functions for S_X, S_Y, S_Z.

0020-1669/87/1326-2191$01.50/0

$$g_X = g_e(A^2 - B^2 - C^2) - 4KBC \quad (3a)$$

$$g_Y = g_e(A^2 - B^2 + C^2) - 4KAC \quad (3b)$$

$$g_Z = g_e(A^2 + B^2 - C^2) - 4KAB \quad (3c)$$

$$A_{(X)} = P[(D - E)^2 + F^2 - 2(D - E)F \cos 4\varphi]^{1/2} \quad (4a)$$

$$A_{(Y)} = P[(D + E)^2 + F^2 + 2(D + E)F \cos 4\varphi]^{1/2} \quad (4b)$$

$$A_{(Z)} = P[-4KAB - \varkappa(1 - 2C^2) + 2(1 + C^2)/7 + 6(A - B)C/7] \quad (4c)$$

where $D = -2K(A + B)C - (7\varkappa + 1)(A^2 - B^2)/7 - 3(A + B)C/7$, $E = -2K(A - B)C - (7\varkappa - 2)C^2/7 + 3(A - B)C/7$, $F = 3(A + B)^2/7$, $P = g_e g_n \beta_e \beta_n \langle r^{-3} \rangle N^2 = 32.9 \times 10^{-4} N^2$ cm^{-1} (N^2 is a covalency factor),[7,9] $g_e = 2.0023$, $\varkappa = 0.35$,[7] and K is an orbital correction factor.[10]

We see from (4a) and (4b) that $A_{(X)}$ and $A_{(Y)}$ vary with φ. A numerical calculation shows, e.g. for **1**, that the ratio $A_{(X)}/A_{(Y)}$ decreases from 13.0 to 0.22 with increase in φ from 0 to 45°. Such large angular dependence affords a basis for interpreting the observed differences and determining the angle φ with considerable accuracy.[11] In practice, (3a)-(3c) are first solved simultaneously for A, B, C, and K, which are then used to solve (4a) and (4b) for φ and N^2. Finally, φ_g, φ_A, and $A_{(Z)}$ are calculated from (1), (2), and (4c), respectively.[12] The orbital reduction factor k is obtained through the approximation $k = (1 + N^2)/2$. In solving (3a)-(3c), we obtained two different solutions with a reasonable value of K depending upon the sign of the **g** tensor determinant, $g_X g_Y g_Z$. However, the solution from $g_X g_Y g_Z < 0$ is incompatible with the observed $A_{(i)}$ values.[13] Hence, the sign of $g_X g_Y g_Z$ must be positive, which is in agreement with the results from Mössbauer data on cytochromes c_2 and P-450.[14] The calculated results for **1** and **2** are given in Table I, where the principal hf values $A_{i'}$ ($i' = X', Y', Z'$) are also listed.

According to a point-charge-model calculation,[15] the angle φ is expressible as a function of rotational orientation angle of axial ligand(s). For complexes with two equivalent axial ligands (e.g. for **1**), $\varphi = (\varphi_1 + \varphi_2)/2$, where φ_1 and φ_2 are the orientation angles of the two axial ligand planes (e.g. the Fe-O-C planes in **1**). In cases where the field strength of one axial ligand dominates over that of the other (e.g. in **2**), $\varphi \simeq \varphi_1$, where φ_1 is the angle of the axial ligand plane with stronger field (e.g. the Fe-S-C plane in **2**). The values $\varphi = 39.7$ and 11.4° determined for **1** and **2** can be discussed on this basis. On the other hand, X-ray and MO calculation studies have shown that two major factors, namely, steric and electronic effects, influence the axial ligand orientation.[2] The rhombic field orientation is affected similarly and the observed angles are the results of the competition of the two effects.

The parameters φ_g, φ_A, N^2, k, and K/k in Table I cannot be assessed without the hf splitting data. Some of them merit comparison between **1** and **2**. The covalency factor N^2 is found to fall in the range allowable for t_2 orbitals of the type $t_2 = N(d\epsilon - \lambda\psi_{lig})$. The larger value of N^2 for **1** compared with that for **2** is consistent with the general trend of Fe-OR and Fe-SR bonds. By contrast, the value K/k is smaller in **1** than in **2**. Since K/k is a measure of the mixing in of excited $t_2^4e\ ^2T_2$,[10] the result is suggestive of the excited states lying higher in **1** than in **2**.

Table I. Summary of Observed and Calculated Results for ^{57}Fe(TPP)(OMe)$_2^-$ (**1**) and ^{57}Fe(TPP)(SEt)(MeOH) (**2**)

	low-spin complex	
	1[a]	**2**
$\lvert g_X \rvert$	1.915	1.958
$\lvert g_Y \rvert$	2.164	2.211
$\lvert g_Z \rvert$	2.491	2.339
$A_{(X)}/G$[b]	6.0	18.2
$A_{(Y)}/G$[b]	16.0	5.5
$A_{(Z)}/G$[b,c]	~9 (9.20)[f]	≲6 (4.78)[f]
$g_X g_Y g_Z$	>0	>0
A	0.99217	0.99647
B	-0.114 76	-0.070 05
C	-0.049 37	-0.046 33
K	1.0945	1.2366
$\varphi = -\varphi_g$/deg[d]	39.66	11.35
φ_A/deg[d]	35.52	6.70
N^2	0.8344	0.6588
k	0.9172	0.8294
K/k	1.1933	1.4910
$A_{X'}/10^{-4}$ cm^{-1}[e]	-16.70	-17.49
$A_{Y'}/10^{-4}$ cm^{-1}[e]	-3.36	1.78
$A_{Z'}/10^{-4}$ cm^{-1}[e]	10.70	5.22

[a] The deuterium-substituted species. See the caption to Figure 1. [b] Normalized by $\lvert g_i \rvert \beta_e$. [c] The line width of g_Z absorption was 2-3 times as broad as those of g_X and g_Y absorptions, which led to less accurate determination of $A_{(Z)}$. [d] The four different angles (e.g. $\pm\varphi$, $90 \pm \varphi$) yield equivalent results. [e] The principal hf values are calculated from $A_{X'} + A_{Y'} = 2PD$, $A_{X'} - A_{Y'} = -2P(E^2 + F^2 + 2EF \cos 4\varphi)^{1/2}$, and $A_{Z'} = A_{(Z)}$. [f] Calculated from (4c). See ref 12.

The present method of hf analysis is of general application to low-spin Fe(III) heme complexes, provided that hf splitting values are experimentally available. For complexes with broad line width, ENDOR spectroscopy would be more suitable. Magnetic Mössbauer spectroscopy can provide a similar electronic characterization. The details have been reported previously.[16]

In sum, it has been demonstrated that a wealth of information is available from the ^{57}Fe hf splitting data. The orientation angle of the rhombic field may serve to probe a delicate electronic and/or structural modulation caused by weak interactions between axial ligands and their surroundings. Further studies of the series of complexes Fe(TPP)(SR)L, where R = *n*-Pr, *n*-Bu, *t*-Bu, C_6H_5, 4-*t*-Bu-C_6H_4, etc. and L = MeOH, RSH, etc., are now in progress, in an attempt to shed light on factors governing the rhombic field orientation.

(9) The covalency effect is taken into consideration with t_2 orbitals of the type $t_2 = N(d\epsilon - \lambda\psi_{lig})$, where $d\epsilon = d_{yz}, d_{zx}, d_{xy}$.
(10) K is related to an orbital reduction factor k ($= 1 - N^2\lambda^2/2$) through $K \simeq k[1 + 6B(3/E_1 - 1/E_2)] \simeq k(1 + 12B/E)$, where E_1, E_2, or E is the energy of excited $t_2^4e\ ^2T_2$ relative to the ground $t_2^5\ ^2T_2$. For details, see: Hill, N. J. *J. Chem. Soc., Faraday Trans. 2* **1972**, *68*, 427. Sato, M.; Ohya, T.; Morishima, I. *Mol. Phys.* **1981**, *42*, 475.
(11) A computer simulation that assumes the random orientation of rhombic field has failed to reproduce the observed spectra for both **1** and **2**, implying that there is a preferred orientation angle φ to be determined.
(12) The calculated value $A_{(Z)}$ is used to justify the validity of the crystal field model on which the present analysis is based.
(13) For **1**, $A = 0.614\,33$, $B = -0.579\,93$, $C = -0.535\,04$, and $K = 1.1474$. The calculated hf splittings are $A_{(X)} = 35.15$-35.12 G, $A_{(Y)} = 32.73$-32.70 G, and $A_{(Z)} = 30.81$ G for $\varphi = 0$-45° and $N^2 = 0.8344$, where the values $A_{(i)}$ are normalized by $\lvert g_i \rvert \beta_e$.
(14) Huynh, B. H.; Emptage, M. H.; Münck, E. *Biochim. Biophys. Acta* **1978**, *534*, 295.
(15) The point-charge approximation is not a good description of the crystal field effect. Nevertheless, we used the approximation to obtain a concrete if rather naive picture of the angular relation between the rhombic field and axial ligand orientations. The angular relation is regarded as zeroth order.
(16) The Mössbauer method fits all three hf values simultaneously: Rhynard, D.; Lang, G.; Spartalian, K.; Yonetani, T. *J. Chem. Phys.* **1979**, *71*, 3715.

Biophysics Division
Faculty of Pharmaceutical Sciences
Teikyo University
Sagamiko, Kanagawa 199-01, Japan

Tomoko Otsuka
Toshie Ohya
Mitsuo Sato*

Received November 3, 1986

Cross Polarization Magic Angle Spinning ^{31}P NMR Spectra of Some $(R_3P)_2MCl_2$ (M = Pd, Pt) Complexes

Sir:

We have observed from several detailed investigations[1-3] of the thermodynamics of the cis-trans isomerizations of $(R_3P)_2PdX_2$

(1) Redfield, D. A.; Nelson, J. H. *Inorg. Chem.* **1973**, *15*, 12.
(2) Verstuyft, A. W.; Nelson, J. H. *Inorg. Chem.* **1975**, *17*, 1501.
(3) Redfield, D. A.; Nelson, J. H. *J. Am. Chem. Soc.* **1974**, *96*, 6219.

0020-1669/87/1326-2192$01.50/0